

**ASSESSMENT OF HYDROGEN ACCUMULATION BEHAVIOR IN STRESSED Al-Zn-Mg
ALUMINUM ALLOYS BY MEANS OF KELVIN FORCE MICROSCOPY**

*H. Fujihara¹, H. Toda¹, K. Shimizu¹, A. Takeuchi² and K. Uesugi²

¹*Department of mechanical engineering, Kyushu University
744, Motoooka, Nishi-ku, Fukuoka 819-0395, Japan
(2TE16750T@s.kyushu-u.ac.jp)*

²*Japan Synchrotron Radiation Research Institute
1-1-1, Kouto, Sayo-cho, Sayo-gun, Hyogo 679-5198, Japan*

ABSTRACT

Hydrogen is trapped at a variety of microstructures, for example grain boundaries, dislocations and particles. It is thought that hydrogen trapped at trapping sites is redistributed to the other sites under loading and then brittle fracture occurs with hydrogen accumulation. In order to understand hydrogen embrittlement behavior, it is necessary to investigate the time evolution behavior of hydrogen accumulation at each trap site. In the present study, changes in hydrogen distribution are observed under stress using Kelvin force microscopy (KFM) that can visualize hydrogen concentration distribution on material surface at high resolution. Spot-like hydrogen enriched regions are observed on the surface of a material. In addition, hydrogen depleted regions are observed around those enriched regions, and the appearance of hydrogen trap due to particles existing near the material surface is revealed. On the other hand, hydrogen trapped at grain boundary can be visualized. From in this result, it was suggested that crystallographic factors influence hydrogen accumulation. The relationship between initiation and propagation of intergranular crack and hydrogen accumulation under stress will be discussed.

KEYWORDS

Aluminum alloy, Hydrogen embrittlement, Kelvin force microscopy

INTRODUCTION

Hydrogen present in a metal sometimes has significant effects on various properties. Hydrogen in a metal is trapped at a variety of microstructure, for example dislocations and grain boundaries. Grain boundaries, dislocations and micropores are the major trap sites in aluminum alloys. Some researchers considered that hydrogen redistribution and accumulation between these trap sites in a material with loading plays an important role in the brittle fracture behavior. In general, in intergranular fracture and quasi-cleavage fracture, the hydrogen trapped at grain boundaries and dislocations contributes to fracture behavior, respectively. Recently some researchers have shown that the ductile fracture in aluminum alloys is resulted from growth and coalescence of hydrogen micropores. Analysis using first principles calculation indicates that intergranular fracture occurs when hydrogen concentration reaches 20 atomH/nm² on grain boundary. From this report, it is considered that hydrogen redistributed during deformation accumulates locally in order to cause hydrogen brittle fracture. In order to understand hydrogen embrittlement, it is necessary to investigate the time evolution behavior of hydrogen accumulation at each trap site. In the present study, we evaluate the relationship between hydrogen accumulation behavior and fracture behavior in Al-Zn-Mg based alloys. In-situ observation was made by combining the tensile test with Kelvin force microscope (KFM) that can visualize the hydrogen concentration distribution on the material surface with high resolution. We also investigate the relationship between hydrogen distribution behavior and crystal orientation.

EXPERIMENTAL

Material

The materials used in present study were an as-rolled modified 7150 aluminum alloy (with 10 mass% Zn) and an as-rolled Al-Zn-Mg ternary alloy (10 mass% Zn, 1.2 mass% Mg). Some heat treatment processes were applied on this material: homogenization and solution treatment followed by aging. Figure 1 shows the optical microstructure of two alloys used in present study.

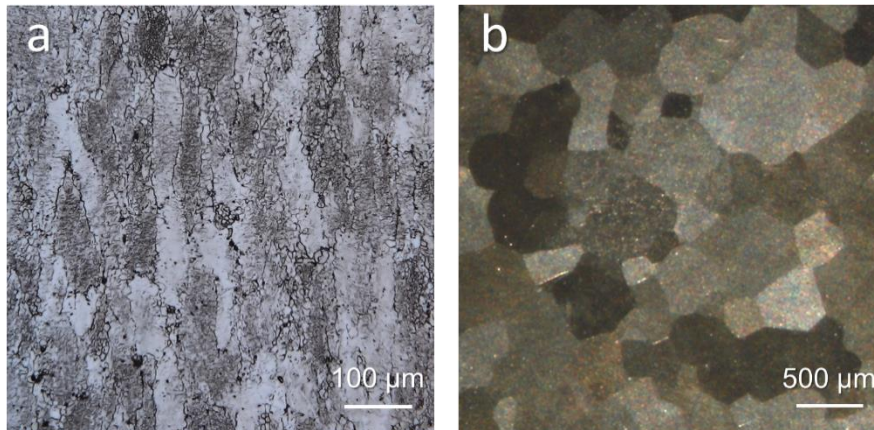


Figure 1. Optical micrographs of (a) modified 7150 aluminum alloy and (b) Al-Zn-Mg ternary alloy

The specimens having gauge length 0.7 mm and cross sectional area 0.6×0.6 mm were used for the in-situ tensile test as shown in Figure 2. All the specimens were prepared by an electro discharge machine (EDM). Hydrogen was charged in the materials during EDM. The specimens were stored in acetone after EDM. After EDM cutting, specimen surface was prepared with mechanical polishing using emery paper and finish polishing with colloidal silica for 30 minutes.

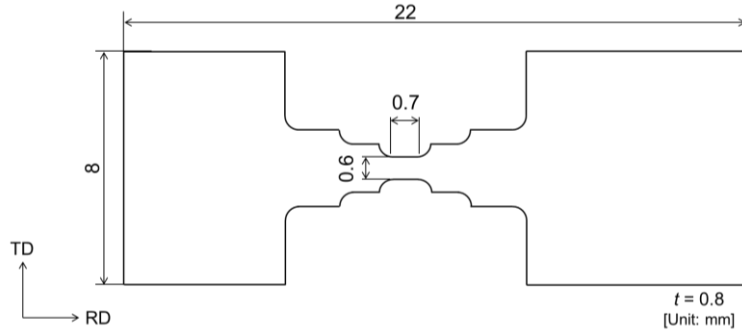


Figure 2. Specimen geometry for in-situ tensile test

Electron Backscatter Diffraction Pattern (EBSD)

Crystal orientations were observed by means of Electron backscatter diffraction pattern (EBSD) measurements. EBSD maps were obtained for Normal Direction (ND) with accelerating voltage of 15 kV.

In-situ Tensile Test

The in-situ tensile test was carried out at beamline BL20XU in SPring-8. The observation was performed by means of a monochromatic X-ray beam which is generated by a liquid nitrogen-cooled Si (111) double-crystal monochromator with a photon energy of 20 keV. The distance from the specimen to the detector was 20 mm. Total 1800 radiographs were scanned for 180 degrees in increments of 0.1 degree. In order to observe the initiation and growth of quasi-cleavage cracks, a tensile test was conducted with a holding time of 8.9 minutes. In addition, when cracks occur and grow to about 30 μm , the specimen was removed from tensile testing machine.

Kelvin Force Microscope (KFM)

KFM can observe the local potential difference of specimen surface with a spatial resolution below 100 nm. The determination of surface potential at a certain point by KFM is given by applying a DC voltage and minimizing electrostatic force between probe and sample. Feedback control is performed so as to minimize the electrostatic force at all times, as a result, a surface potential map is created. The relationship between the presence of hydrogen and the surface potential is in accordance with the Nernst equation:

$$E = E_{\text{SHE}}^0 + RT/F \ln(a(\text{H}_{\text{el}}^+)/a(\text{H}_{\text{ad}})) \quad (1)$$

where E , E_{SHE}^0 , R , T , F , $a(\text{H}_{\text{el}}^+)$, $a(\text{H}_{\text{ad}})$ is potential differences, standard hydrogen electrode potential, gas constant, temperature, Faraday constant, the activity of hydrogen ions in the electrolyte, the activity of adsorbed hydrogen. Therefore, the surface potential becomes lower as the hydrogen concentration increases. Furthermore, observing the same region continuously, it is possible to directly visualize the diffusion and accumulation behavior of hydrogen. On the other hand, care should be taken because the surface topology significantly affects the obtained surface potential image. The KFM measurements in present study were performed using Agilent 5400 SPM as shown in Figure 3. For the probe, PtIr-coated Si chip was used. This probe has a tip radius of curvature of 25 nm with a resonance frequency of 75 kHz. Measurement is carried out using tapping mode, and in addition to the surface potential, surface topology can be obtained at the same time. A tensile strain was applied to the specimen, and observation was performed at the characteristic point such as grain boundary. Also, in order to reduce the influence of environmental hydrogen, observation was performed in a nitrogen gas atmosphere.

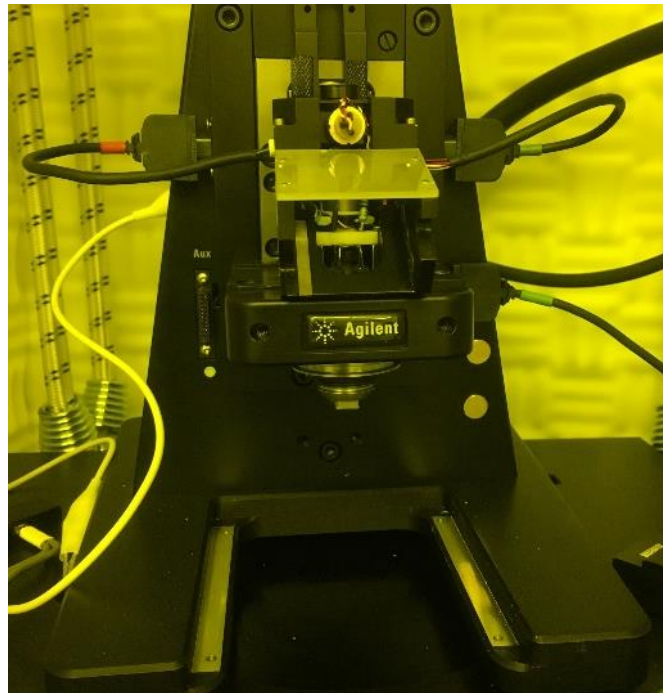


Figure 3. The KFM device

RESULTS AND DISCUSSION

The potential in the vicinity of a crack for the 7150 alloy with the quasi-cleavage crack was observed by KFM from the tensile strain to 4%. Figure 4 shows the observation results of KFM in the region which is 100 μm far from the crack tip. The topology images and the potential images were elapsed when 1 and 4 hours after applying tensile strain, respectively. Contrast corresponding to the surface topology on the grain boundary when applying the strain was observed in the potential image (Figure 4a' and 4b'). However, it was observed that the potential changes on several grain boundaries. From this result, the change in these potential images were caused by accumulated hydrogen. In addition, observation results of KFM in the region which is 75 μm far from the crack tip was performed. Also in this observed region, the contrast corresponding to the surface topology and the change on the grain boundary were observed with time in the same manner. Such behavior was observed at specific grain boundaries, and the different behavior caused by misorientation has been shown. The potential changes on the grain boundaries at each location are different, and at 75 and 100 μm , the potential increases and decreases with time were observed, respectively.

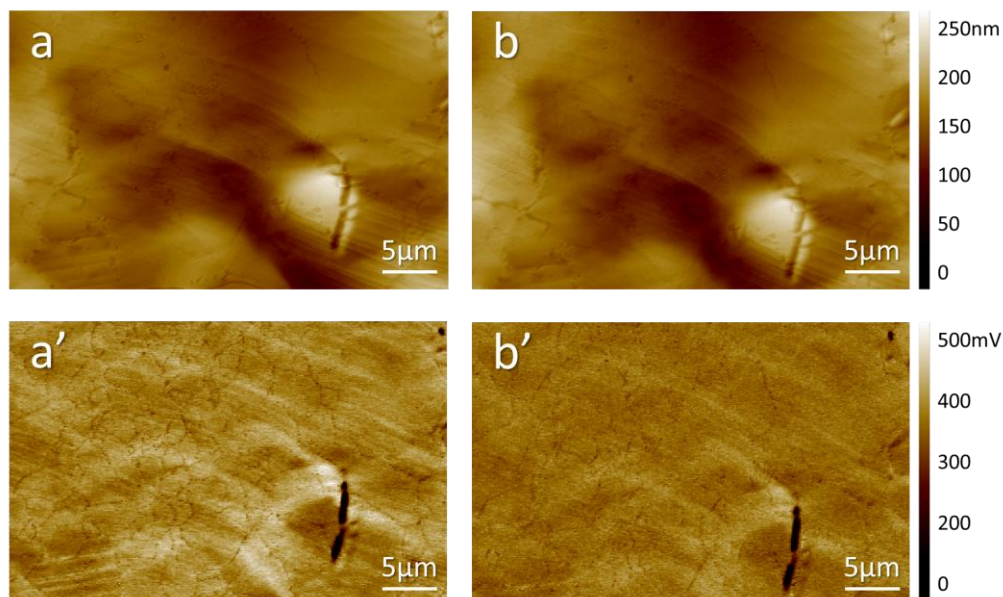


Figure 4. Surface topology images and potential images near crack tip field with 4% strain taken after (a, a') 1 and (b, b') 4h from loading

For ternary Al - Zn - Mg alloys with tensile strain of 4%, the potential was observed using KFM around triple junctions. In addition to the potential contrast caused by the surface topology, a reduction in potential, that is to say, accumulation of hydrogen on the grain boundary was clearly appeared. On the other hand, KFM observation was made at an intergranular crack tip. The state of hydrogen accumulation around the crack tip was not observed, and as a result of additional loading, it was observed that this crack had propagated into the grain.

To the ternary alloy having a notch radius 100 μm at the center of specimen after giving the strain of 4% was observed potential by KFM. On the surface of material, spot-like hydrogen enriched regions were observed. In addition, hydrogen depleted regions are observed around those regions, and the appearance of hydrogen trap due to particles existing near the material surface is revealed.

CONCLUSIONS

The hydrogen accumulation and diffusion behavior in the Al-Zn-Mg based alloy has been investigated by means of Kelvin force microscopy combined with tensile test. For the specimens applied tensile strain, it was observed that hydrogen accumulated at specific grain boundaries. It was shown the hydrogen accumulation behavior caused by misorientation. In addition, it was revealed that hydrogen was trapped in particles, and hydrogen was depleted around them, suggesting that there is a relationship between the stress state and hydrogen accumulation.

ACKNOWLEDGMENTS

This research was supported by the Heterogeneous Structure Control, Towards Innovative Development of Metallic Structural Materials, from Japan Science and Technology Agency, JST. The synchrotron radiation experiments were performed at SPring-8 with the approval of JASRI through Proposal No. 2017B0076

REFERENCES

- Birnbaum, H. K., & Sofronis, P. (1994). Hydrogen-enhanced localized plasticity—a mechanism for hydrogen-related fracture. *Materials Science and Engineering: A*, *176*(1–2), 191–202. [https://doi.org/10.1016/0921-5093\(94\)90975-X](https://doi.org/10.1016/0921-5093(94)90975-X)
- Evers, S., & Rohwerder, M. (2012). The hydrogen electrode in the “dry”: a Kelvin probe approach to measuring hydrogen in metals. *Electrochemistry Communications*, *24*, 85–88. <https://doi.org/10.1016/j.elecom.2012.08.019>
- Koyama, M., Rohwerder, M., Tasan, C. C., Bashir, A., Akiyama, E., Takai, K., & Tsuzaki, K. (2017). Recent progress in microstructural hydrogen mapping in steels: quantification, kinetic analysis, and multi-scale characterisation. *Materials Science and Technology*, *33*(13), 1481–1496. <https://doi.org/10.1080/02670836.2017.1299276>
- Larignon, C., Alexis, J., Andrieu, E., Lacroix, L., Odemer, G., & Blanc, C. (2013). Combined Kelvin probe force microscopy and secondary ion mass spectrometry for hydrogen detection in corroded 2024 aluminium alloy. *Electrochimica Acta*, *110*, 484–490. <https://doi.org/10.1016/j.electacta.2013.02.063>
- Toda, H., Inamori, T., Horikawa, K., Uesugi, K., Takeuchi, A., Suzuki, Y., & Kobayashi, M. (2013). Effects of hydrogen micro pores on mechanical properties in A2024 aluminum alloys. *Materials Transactions*, *54*(12), 2195–2201. <https://doi.org/10.2320/matertrans.L-M2013832>
- Toda, H., Oogo, H., Horikawa, K., Uesugi, K., Takeuchi, A., Suzuki, Y., Nakazawa, M., Aoki, Y., & Kobayashi, M. (2014). The True Origin of Ductile Fracture in Aluminum Alloys. *Metallurgical and Materials Transactions A*, *45*(2), 765–776. <https://doi.org/10.03.239/s11661-013-2013-3>